

DISCOVERY OF TWO NEW, CARBON-RICH PROTO-PLANETARY NEBULAE: IRAS Z02229 + 6208 AND IRAS 07430 + 1115

BRUCE J. HRIVNAK¹

Department of Physics and Astronomy, Valparaiso University, Valparaiso, IN 46383; bhrivnak@exodus.valpo.edu

AND

SUN KWOK^{1,2}

Department of Physics and Astronomy, University of Calgary, Calgary, Alberta, Canada T2N 1N4; kwok@iras.ucalgary.ca

Received 1998 April 27; accepted 1998 October 15

ABSTRACT

We report the discovery of two new carbon-rich proto-planetary nebulae (PPNs), IRAS Z02229 + 6208 and 07430 + 1115. Optical spectroscopy of these sources and another previously discovered PPN, IRAS 05431 + 0852, reveals the presence of C₂ and C₃ in absorption. All three objects have the spectra of G–K supergiants, consistent with the expectations of their being PPNs. New ground-based optical and infrared photometry, combined with the *IRAS* measurements, show double-peak spectral energy distributions for each; this suggests that the asymptotic giant branch (AGB) mass loss has ended and these objects are in the post-AGB phase of evolution. The remnant of the molecular envelope is detected in CO emission for the first time in all three objects, using the CO (3–2) line. The 3.3 and 11.3 μm emission features commonly attributed to the polycyclic aromatic hydrocarbon molecules have been detected in IRAS 07430 + 1115. Strikingly absent in IRAS 07430 + 1115, however, is the 21 μm emission feature, found in the other two and in all but one of the other PPNs known to show C₂ in absorption.

Subject headings: circumstellar matter — infrared: stars — stars: post-asymptotic giant branch — supergiants

1. INTRODUCTION

The evolutionary phase between the end of the asymptotic giant branch and the beginning of the planetary nebula phase has long been a missing link in our understanding of the late stages of stellar evolution. Objects in this transitional phase, called proto-planetary nebulae (PPNs), are difficult to identify because their nebulosities are faint and they often have optical appearances similar to those of stars. However, the last decade has witnessed the identification of several dozen PPNs. These objects were initially identified on the basis of their infrared excesses in the *IRAS* database and then confirmed through ground-based follow-up observations. Their spectral energy distributions show a characteristic double-peak shape, with emission in the visible and near-infrared region coming from the reddened photosphere and emission in the mid- and far-infrared from the optically thin circumstellar dust shell. The spectra of the central stars range in types from B to late G and show the luminosity characteristics of supergiants. Molecular envelopes are detected around the objects, expanding at typical velocities of 10 to 20 km s⁻¹. Summaries of their observational properties can be found in Kwok (1993) and Hrivnak (1997).

In a recent paper we identified a group of these objects as carbon rich, based on the presence of molecular carbon in their optical spectra (Hrivnak 1995). This is supported by

the presence and relative strength of HCN in their millimeter-wavelength spectrum (Omont et al. 1993). An interesting and important correlation has been found between the presence of molecular carbon in the optical spectrum and the presence of a strong, unidentified emission feature at 21 μm in the mid-infrared spectrum. The 21 μm emission feature has been identified in 11 objects to date, all of which are PPNs. Molecular carbon absorption features are seen in the optical spectra of all of these but one, the very faint (*V* = 24), heavily obscured source IRAS 22574 + 6609, for which optical spectroscopy is difficult to obtain. In addition, each of these PPNs with molecular carbon and the 21 μm emission feature also possesses an emission feature at 3.3 μm, attributed to polycyclic aromatic hydrocarbons (PAHs); some also possess an additional emission feature at 3.4 μm (Hrivnak 1997).

In this paper, we discuss two new PPNs that possess molecular carbon in their optical spectra, IRAS Z02229 + 6208 and 07430 + 1115, along with 05341 + 0852, for which molecular carbon has been independently found by Reddy et al. (1997). We will present a variety of observations, which support the identification that these are carbon-rich PPNs.

2. IDENTIFICATION OF THE SOURCES

The identification of IRAS Z02229 + 6208 deserves a bit of explanation, because the object is not found in the *IRAS* Point Source Catalog (PSC), even though it is bright. It was found when one of us (B. J. H.) was systematically examining the *IRAS* Faint Source Survey (FSS) database for sources that peak in the 25 μm band, such that $F_{12} < F_{25}$ and $F_{25} > F_{60}$. This was carried out using the database at NASA's Infrared Processing and Analysis Center (IPAC) in Pasadena. The FSS database consists of the Faint Source Catalog (FSC) and the Faint Source Reject File (FSR), in

¹ Visiting Astronomer, Kitt Peak National Observatory, National Optical Astronomy Observatories, operated by the Association of Universities for Research in Astronomy, Inc., under contract with the National Science Foundation.

² Visiting Astronomer, James Clerk Maxwell Telescope, which is operated by the Joint Astronomy Centre on behalf of the Particle Physics and Astronomy Research Council of the United Kingdom, the Netherlands Organization for Scientific Research, and the National Research Council of Canada.

TABLE 1
SOURCE POSITIONS AND *IRAS* FLUXES

<i>IRAS</i> Identification	R.A. (2000)	Decl. (2000)	<i>l</i> (deg)	<i>b</i> (deg)	F_{12} (Jy)	F_{25} (Jy)	F_{60} (Jy)	F_{100} (Jy)
02229+6208.....	02:26:41.77	+62:21:22	133.7	1.5	66.7	203.6	30.6	...
05341+0852.....	05:36:55.00	+08:54:08	196.2	-12.2	4.5	9.9	3.7	3.8
07430+1115.....	07:45:51.39	+11:08:19	208.9	17.0	7.6	30.3	9.9	2.5

addition to actual sky images (“Plates”), which were not used in this study. The FSS goes approximately a factor of 2.5 times fainter than the PSC; this is accomplished by co-adding the data before they are extracted. By going fainter, confusion becomes more of a problem, and so the FSC excludes objects with galactic latitude $|b| < 10^\circ$. The FSC is only somewhat less reliable than the PSC, 98.5% versus 99.997% (Mosher et al. 1992). The FSR contains objects in this region of greater confusion, $|b| < 10^\circ$, as well as less reliable detections from around the sky.

IRAS Z02229+6208 was found in the FSR (thus the “Z” designation), where it stood out because it is so bright, $F_{25} = 200$ Jy. This leads to the question of why the source was not included in the *IRAS* PSC. The individual scans of the source were examined at IPAC, with the assistance of Tom Chester. It appears that it failed to meet the PSC criteria of 2 hours confirmed observations (HCONS), because in one of the two possible HCONS, four detectors (rather than the maximum acceptable upper limit of three) in the 12 μm band were lit up; this suggested that it was an extended or a double point source and not a true point source. Examination of a high-resolution map of the *IRAS* data revealed a nearby source almost lined up in the scan direction, which apparently caused the source confusion. We then used software at IPAC to compare the position of the *IRAS* source with sources in the STScI Guide Star Catalog (GSC) and found it to be close to a bright star. We have since confirmed this star to indeed be the optical counterpart on the basis of ground-based imaging at 10 μm .

IRAS 07430+1115 is a PSC source that was identified in a more standard manner, which we have used previously to identify many PPN candidates. The source was initially selected based on its *IRAS* colors. We then transposed its position to the Palomar Observatory Sky Survey prints and found it to be very near a bright star, which we assigned as an optical candidate. We have since identified it in the GSC. This optical association was later confirmed by a ground-based observation at the United Kingdom Infrared Telescope (UKIRT), using a bolometer at 10 μm .

IRAS 05431+0852 was identified by Geballe & van der Veen (1990) as a PPN candidate. They obtained infrared photometry of the object and noted its optical counterpart.

The coordinates of these three objects, taken from the STScI GSC, are listed in Table 1, along with their *IRAS* fluxes. The fluxes for *IRAS* 07430+1115 and 05341+0852 are from the FSC. For *IRAS* Z02229+6208, there is background contamination from a nearby bright H II region; the source happens to lie near the northern extent of the bright H II region W3 (W3N). We therefore manually extracted the flux measurements using the IPAC program ADDSCAN and obtained very good measurements in the 12 and 25 μm bands and a good measurement in the 60 μm bands; the 100 μm measurement is overwhelmed by the nearby bright source. In Figure 1 we display finding charts for these three sources.³

3. OBSERVATIONS

3.1. Optical and Infrared Photometry

CCD imaging of these objects was carried out on several nights at the Kitt Peak National Observatory (KPNO). The 0.9 m telescope was used in the direct imaging mode, with standard “Harris” *BVRI* filters. Standard stars from the list of Landolt (1983) were observed and used to derive extinction and transformation coefficients. The reductions were carried out within IRAF⁴ and magnitudes derived from aperture photometry using DAOPHOT within IRAF. The standard magnitudes of these objects are listed in Table 2, along with the observing dates. Note that the objects are very red, with $B-V$ of 2.83, 1.81, and 1.86 for *IRAS*

³ Note that in the small finding chart published by Reddy & Parthasarathy (1996), they appear to have incorrectly identified 05341+0852 with the brighter star 1.5 north of the object.

⁴ The Image Reduction and Analysis Facility (IRAF) is distributed by the National Optical Astronomy Observatories, which is operated by the Association of Universities for Research in Astronomy, Inc., under contract to the National Science Foundation.

TABLE 2
OPTICAL AND NEAR-INFRARED PHOTOMETRY RESULTS

<i>IRAS</i> Identification	<i>B</i>	<i>V</i>	<i>R</i>	<i>I</i>	Observation Date
02229+6208.....	14.92 \pm 0.03	12.09 \pm 0.03	10.41 \pm 0.03	8.92 \pm 0.03	1993 Oct 27
05341+0852.....	15.36 \pm 0.02	13.55 \pm 0.02	12.46 \pm 0.02	11.43 \pm 0.02	1995 Sep 13
07430+1115.....	14.48 \pm 0.02	12.62 \pm 0.02	11.63 \pm 0.02	10.69 \pm 0.02	1993 Oct 27
<i>IRAS</i> Identification	<i>J</i>	<i>H</i>	<i>K</i>	<i>L</i>	Observation Date
02229+6208.....	6.66 \pm 0.02	5.33 \pm 0.03	5.46 \pm 0.02	4.90 \pm 0.04	1993 Nov 9, 10
05341+0852.....	10.01 \pm 0.02	9.42 \pm 0.02	9.12 \pm 0.02	...	1995 Oct 10
07430+1115.....	8.84 \pm 0.03	8.23 \pm 0.02	7.83 \pm 0.02	7.3 \pm 0.2	1993 Nov 9, 10

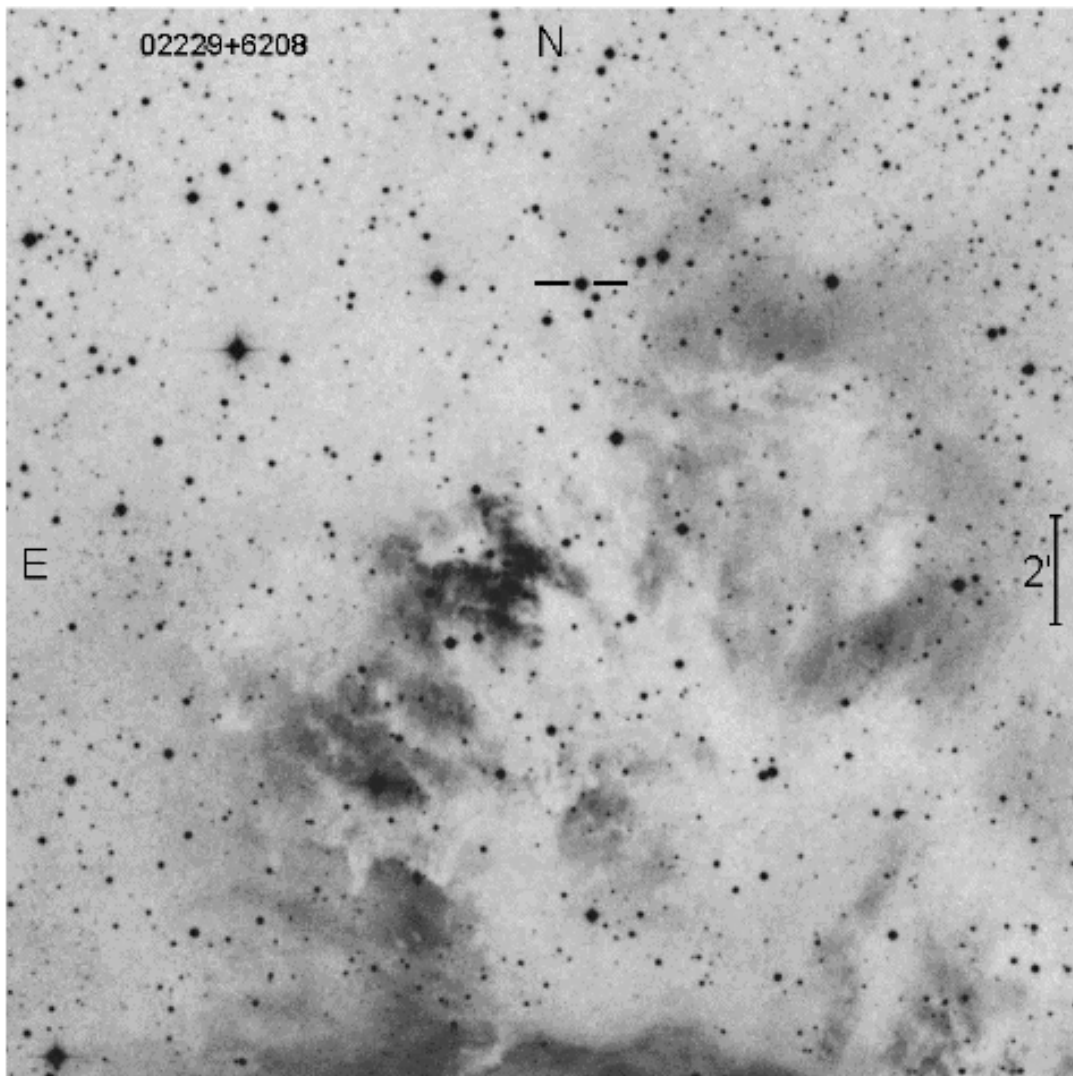
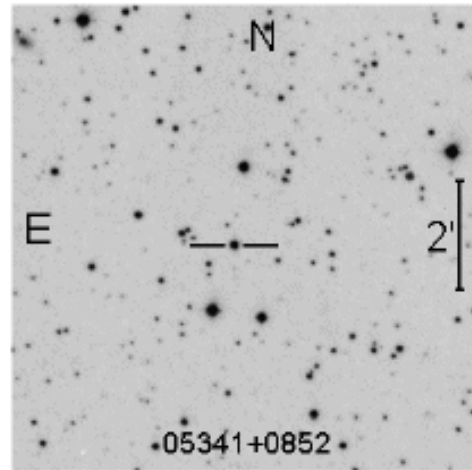
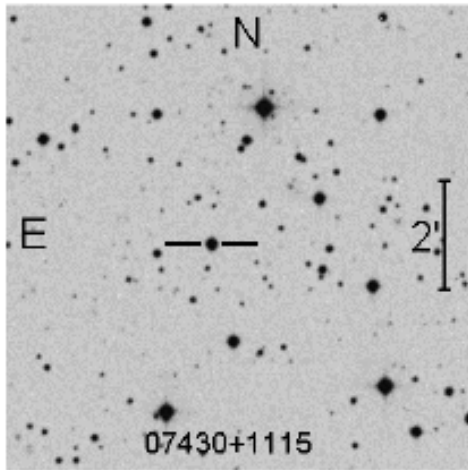


FIG. 1.—Digitized sky survey fields showing the optical counterparts of IRAS Z02229 + 6208, 05341 + 0852, and 07430 + 1115

Z02229+6208, 05341+0852, and 07430+1115, respectively. The images of the PPNs were examined for evidence that they were extended. Unfortunately, the seeing was poor on several of the nights. There is a suggestion that IRAS Z02229+6208 is extended in $H\alpha$; it had an image size of $2''.0$ compared with $1''.8$ for the field stars. However, through the V filter it was the same size as field stars, $1''.6$, and, similarly, observations through the other broadband filters gave no evidence that it was extended. IRAS 07430+1115 was not extended when observed with the poor seeing of $2''.8$, and IRAS 05341+0852 was not extended at a seeing of $1''.5$.

We note that the published magnitudes of IRAS 05341+0852 by Reddy & Parthasarathy (1996) appear to be in error. They claim $V = 11.89$ and $B - V = 0.61$ on measurements made in 1993 January. We have made a V measurement of the object in 1993 October, 2 yr prior to the one given in Table 2, and obtained exactly the same result as in Table 2, $V = 13.55$. Photometric monitoring of this object from 1994 through 1996 shows variability of less than 0.1 mag. Also, the color of their measurement is very different from ours. We noted earlier that their finding chart appears to incorrectly identify 05341+0852 with a star 1.5 north of the correct object. We measured the V magnitude of that star and find it to agree with their published value, listed above. Thus, it appears that they incorrectly identified the star and that the resultant magnitudes do not apply to IRAS 05341+0852.

Near-infrared photometric observations of IRAS Z02229+6208 and 07430+1115 were made with the KPNO 1.3 m telescope on 1993 November 9–11. The Simultaneous Quad-color Infrared Imaging Device (SQIID), which uses four 256×256 PtSi detectors, was used to obtain images at the J , H , K , and L bands simultaneously. The pixel size corresponds to $1''.4$ on the sky, with a field of view of 1° . IRAS 05341+0852 was observed at KPNO using the Cryogenic Optical Bench (COB) on the 2.1 m telescope, on 1995 October 10. COB has a 256×256 pixel InSb detector, and at the focal scale of the 2.1 m telescope it has the much smaller pixel size of $0''.2$. The images were flat-fielded and sky subtracted using IRAF, and magnitudes were derived from aperture photometry using DAOPHOT within IRAF. The magnitudes were corrected for atmospheric extinction and transformed to the standard system, using standard stars from the lists of Elias et al. (1982). These results are also listed in Table 2. Images of Z02229+6208 clearly revealed that it was extended in the near-infrared.

IRAS 07430+1115 was observed with a bolometer at the 3.8 m UKIRT on 1993 March 6, as part of their service observing program. A $10 \mu\text{m}$ measurement of $N = 1.80 \pm 0.05$ was made, which agrees well with the IRAS $12 \mu\text{m}$ flux.

The spectral energy distribution (SED) for each of the three stars is shown in Figure 2. The SED is clearly made up of two components, a reddened stellar photosphere and a dust envelope. For IRAS 05341+0852, we have included the infrared photometry of Geballe & van der Veen (1990), but not that of Manchado et al. (1989), which shows a discrepant H magnitude and only upper limits at L and M . The variations in the narrowband $10 \mu\text{m}$ photometry for 05341+0852 reflect the strong emission peaks at 8 and $11 \mu\text{m}$ in the mid-infrared spectrum (Kwok, Hrivnak, & Geballe 1995; Justtanont et al. 1996), but the cause of the low value at $20 \mu\text{m}$ is unexplained.

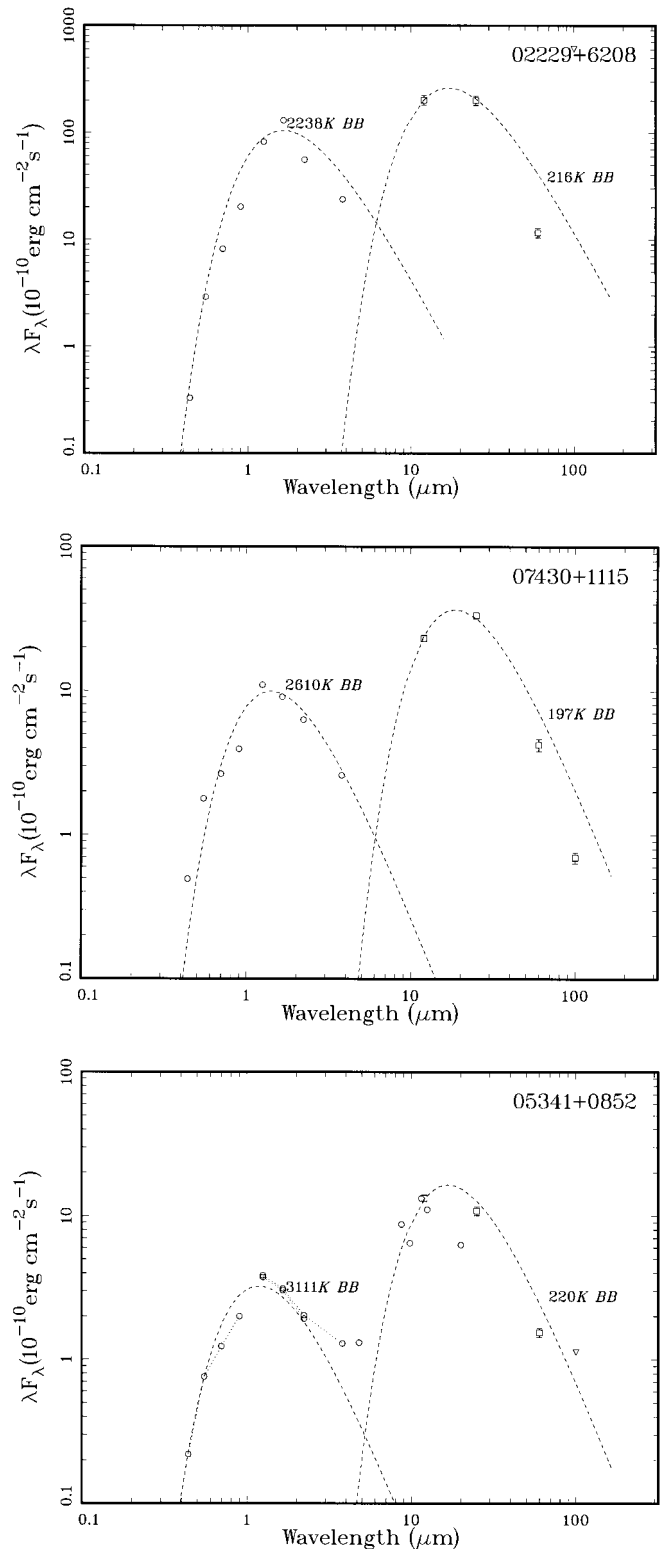


FIG. 2.—SEDs of IRAS Z02229+6208, 07430+1115, and 05341+0852. The open circles and squares are KPNO and IRAS (color-corrected) photometric measurements, respectively. For IRAS 05341+0852, we have included data from Geballe & van der Veen (1990). Two blackbodies are fitted to the photospheric and dust components, with the color temperatures shown above each curve.

3.2. Optical Spectroscopy

Optical spectroscopy was carried out in 1992 October 6–8, using the KPNO 2.1 m telescope. The Gold Camera Cassegrain CCD Spectrometer was used, with a Ford 3K

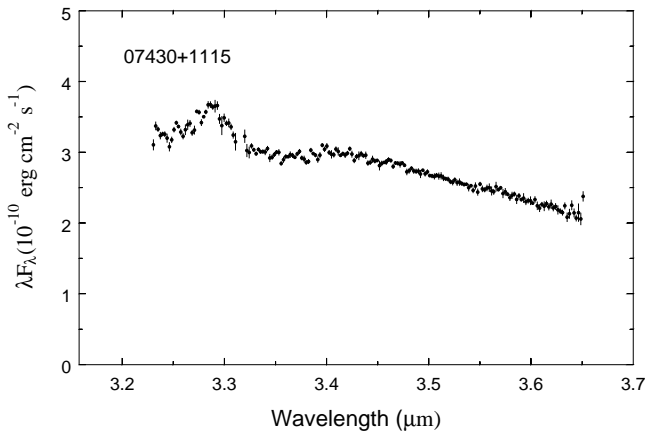


FIG. 3.—UKIRT CGS4 *L*-band spectrum of 07430+1115, showing a 3.29 μm and a weak 3.4 μm emission feature.

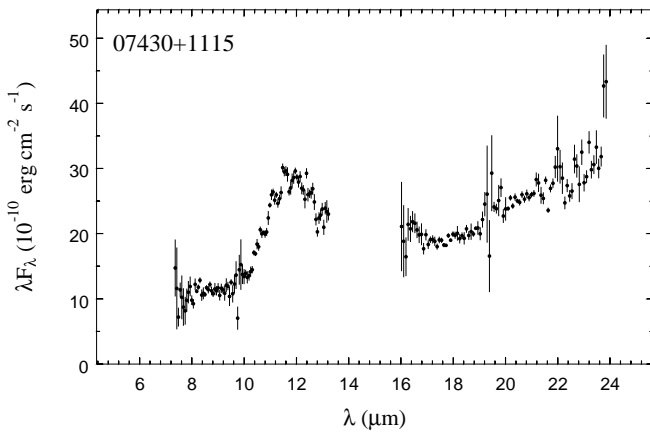


FIG. 4.—UKIRT CGS3 spectrum of 07430+1115, showing an 11–12 μm emission feature but no 21 μm emission feature.

(3200 \times 150 pixel) chip and the “58” grating in the second order. This combination produced a spectrum of almost 2300 \AA in width, with a resolution of 3.1 \AA . Spectra of an He-Ne-Ar arc were taken before and after each stellar spectrum and used for wavelength calibration. The spectra of a number of spectral standards were also obtained for comparison.

The spectra were reduced using IRAF; they were bias subtracted, flat-fielded corrected with the use of a lamp, sky subtracted following cosmic-ray removal, and wavelength calibrated with the use of the arcs, and one-dimensional spectra were extracted. The spectra were not flux calibrated, and the continua shapes include the instrumental system response. There are a few bad columns in the detector, which were noted.

The spectra of all three look like those of cool supergiants, and all three show absorption features due to molecular carbon. These are discussed in detail in § 4.

3.3. Near- and Mid-Infrared Spectroscopy

An *L*-band spectrum of 07430+1115 was obtained at the UKIRT under the service observing program on 1993 November 21 using the facility instrument CGS4. The observations were made in the chop-along-slit/nod mode. CGS4 is a 58 \times 62 InSb array spectrometer and was used in the 75 l mm^{-1} grating mode. A strong emission feature at 3.29 μm can be seen with an indication of a weak feature at 3.4 μm . This is shown in Figure 3. An *H*-band spectrum of this object taken previously showed only hydrogen Brackett lines in absorption (Hrivnak, Kwok, & Geballe 1994).

We were particularly desirous of obtaining mid-infrared spectra of these two new sources to see if they contained the 21 μm emission feature. The *IRAS* LRS spectrum of 07430+1115 was extracted at the University of Calgary; it was assigned a spectral class of “U”, indicating an unusual

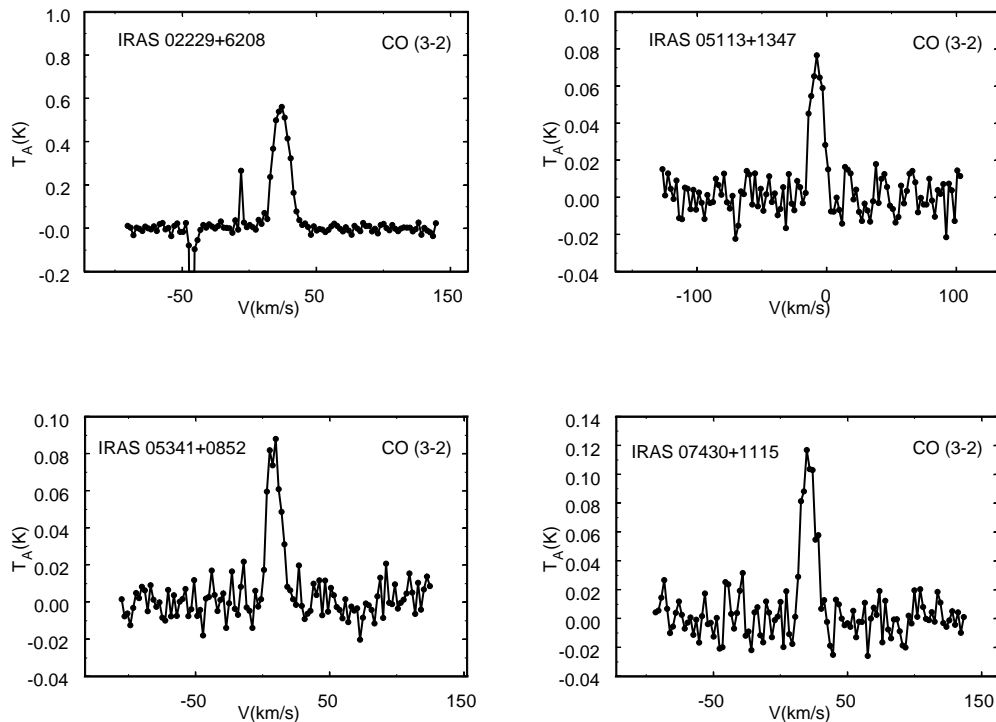


FIG. 5.—CO $J = 3-2$ line for the four new sources. The antenna temperature has been corrected to outside of the Earth’s atmosphere.

spectrum (Kwok, Volk, & Bidelman 1997), and is of poor quality. To obtain better signal-to-noise and spectral resolution, mid-infrared spectra of 07430+1115 were observed at the UKIRT on 1995 March 17, as part of their service observing program. The facility instrument CGS3 was used, which is a 32 channel cooled grating spectrometer covering the spectral range of 7–24 μm . There are two gratings that cover the 10 and 20 μm atmospheric windows, and they produce spectral resolving powers of ~ 50 and ~ 72 , respectively. An aperture of 5" was used, and a 20" north-south chop and nod. A krypton lamp was used for wavelength calibration. The flux was calibrated by comparison with BS 2990, which was assumed to have a temperature of 4750 K and flux values of 125 Jy at 10 μm and 30.5 Jy at 20 μm . Figure 4 shows the CGS3 spectrum of 07430+1115. A strong 11.3 μm PAH feature can be seen, although perhaps at a slightly longer wavelength (11.7 μm). In the 20 μm band, the spectrum shows a strong continuum rising gradually toward the longer wavelengths. There is no obvious evidence for the presence of the 21 μm feature seen in a number of other carbon-rich PPNs (Kwok, Volk, & Hrivnak 1989). Unfortunately, IRAS Z02229+6208 is above the northern declination limit of the UKIRT telescope and thus could not be observed.

3.4. CO Observations

CO emission from IRAS Z02229+6208 was first detected at the James Clerk Maxwell Telescope (JCMT) on 1994 June 23–26 and later reobserved together with IRAS

05113+1347, 05341+0852, and 07430+1115 on 1998 April 9. The observations were taken using a beam switch of 120" in azimuth at 1 Hz. The dual-channel SiS receiver B3 was used together with an autocorrelation spectrometer. The spectrometer bandwidth was 250 MHz, resulting in a channel spacing of 313 kHz and an effective resolution of 378 kHz, i.e., a velocity resolution of 0.33 km s^{-1} at 345.8 GHz. Signals from both polarization channels were averaged together, and the spectra were binned over eight channels, with a resulting velocity resolution of 2.5 MHz, or 2.17 km s^{-1} . The CO (3–2) transition was detected in all four sources. The spectra are shown in Figure 5, and the derived line parameters are given in Table 3.

All these are the first detections of CO in these objects. IRAS 07340+1115 has been searched for CO (1–0) and CO (2–1), but it has not been detected (Nyman et al. 1992; Omont et al. 1993). IRAS 05113+1347 is a similar carbon-rich PPN (Hrivnak 1995), which had not been observed in CO. Note that CO lines in all but IRAS Z02229+6208 are rather weak.

4. DESCRIPTION OF THE OPTICAL SPECTRA

4.1. Classification

The optical spectra of all three sources are shown in Figure 6. They all display the spectra of cool stars, with the G band relatively strong. Also, C_2 absorption is seen in all three, with differing strengths. Judging by the continua levels, IRAS Z02229+6208 appears to be extremely

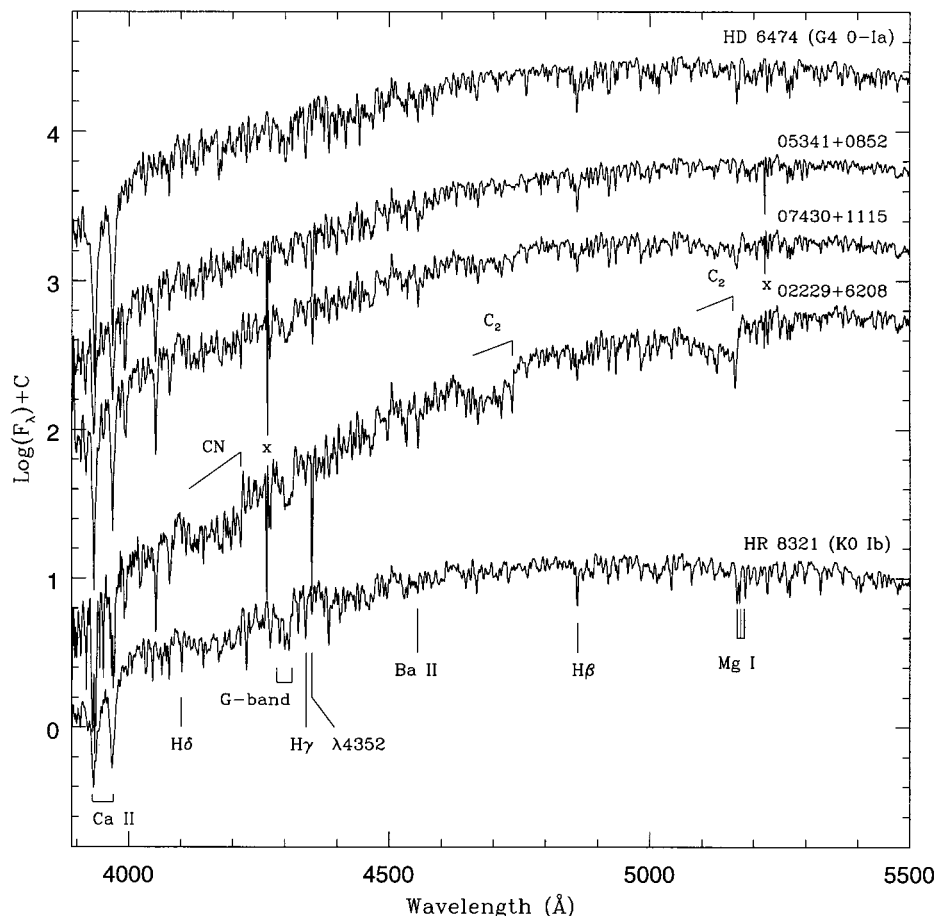


FIG. 6.—Optical spectra of the three sources, along with spectral standards, with the fluxes plotted on a log scale. Note that the fluxes are not calibrated and are simply shifted vertically for plotting purposes. Also note that the sharp lines at $\lambda 4265$ and $\lambda 5220$, indicated with “x”, are due to bad columns on the detector that show up for the fainter program stars.

reddened, which is consistent with the very red color index observed. Several standard stars are included in the figure for comparison.

The spectra were classified using the features discussed and displayed by Keenan & McNeil (1976), Yamashita, Nariai, & Norimoto (1978), and Jaschek & Jaschek (1987). We note at the outset that the spectra of the three objects are difficult to classify due to the presence of molecular carbon features, the apparent enhancement of *s*-process elements (such as Y, Sr, and Ba), and other possible spectral anomalies. In all three, Ca I λ 4226 appears weak and blended with another line at shorter wavelength (or possible infilling by emission), similar to what was observed by Hrivnak (1995) in other C-rich PPNs; this weakness in what would be expected to be a strong line may be evidence of a low abundance of Ca. Also, in all three, λ 4178 is stronger than λ 4172, an unexpected effect again seen in the previously studied C-rich PPNs (Hrivnak 1995), and which we discuss below. In Figure 7 we display spectra of only the shorter wavelength region, showing on an enlarged wavelength scale many of the classification features referred to in this section.

07430+1115.—The strength of the G band suggests an early-G spectral type, while the strengths of the Balmer lines suggest late-G, although we note that any infilling by emission in the Balmer lines would make the star seem cooler. We examined several ratios: Fe I λ 4144/H δ , Fe I λ 4046/H δ ,

and Fe I λ 4272/4290. On the basis of these, we conclude that the spectral type is about G5. The CN band at λ 4216 is evident. The luminosity classification consistently points to a high luminosity class. This is based on the following feature ratios: Sr II 4077/H δ ; Sr II 4077/Fe 4071; Y II, Fe 4376/Fe 4383; Y II, Fe 4442/4435 blend; and Y II 3983/Fe 4005. The G band suggests 0-Ia, especially the λ 4314 line. Fe II 4178/4172 is recommended as a luminosity indicator in G supergiants, with the λ 4178 component strengthening more rapidly with increasing luminosity and increasing temperature. In 07430+1115, λ 4178 is stronger than λ 4172, an effect not seen in any of the standards we observed or the spectral atlases listed above. Most of these luminosity criteria involve *s*-process elements, which appear to be overabundant in this star and thus will affect the luminosity classification. However, based on the above features, we classify the spectrum of the star as G5 0-Ia.

05341+0852.—This star was classified in a similar way to 07430+1115 and appears to be slightly earlier. In 05341+0852, λ 4178 is significantly stronger than λ 4172. We classify it as G2 0-Ia.

Z02229+6208.—This star is clearly cooler than the other two and heavily reddened. The G band is very strong, as is the CN band at λ 4216. These may well be affected by enhanced carbon. Similar criteria as with 07430+1115 were used, plus Fe 4325/H γ . Individual feature ratios give a range of G5 to K3; we assign an average of G8-K0 0-Ia.

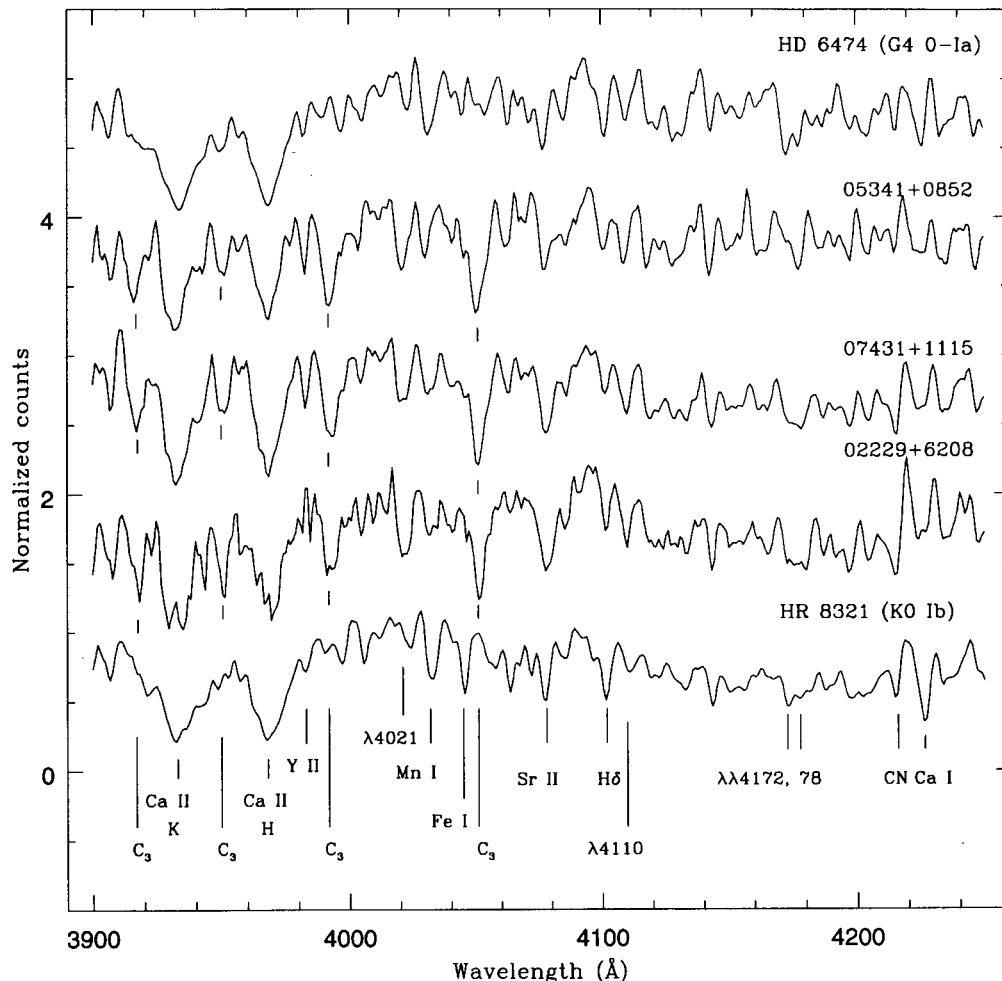


FIG. 7.—Optical spectra, rectified to a continuum level of 1.00 and offset vertically for display purposes. Several of the features discussed in the text are indicated, including the absorption features of C₃. Note that the highly reddened spectrum of Z02229+6208 has a low signal-to-noise ratio in this region.

TABLE 3
OBSERVED CO (3–2) LINE PARAMETERS

Object	Peak T_A (K)	V_{exp} (km s $^{-1}$)	V_{lsr} (km s $^{-1}$)	Integrated Intensity (K km s $^{-1}$)	rms Noise [K(2.5 MHz) $^{-1}$]
02229 + 6208	0.56	15.2	+24.3	8.49	0.015
05113 + 1347	0.077	13.1	–7.5	0.85	0.009
05341 + 0852	0.087	13.1	+9.7	1.00	0.009
07430 + 1115	0.11	15.2	+20.8	1.29	0.012

The classification of all three as very luminous supergiants is based on several features. Two are deserving of particular note. The ratio of Fe II 4178/4172 greater than 1.0 was discussed above and indicated a luminosity class of 0. This may be due to a contribution by Y II 4178. The feature λ 4110 is seen in supergiants and peaks in the spectral range G8–K0, and the ratio λ 4110/H δ increases with higher luminosity and approaches 1.0 at luminosity class 0. In all three of our objects, the line at λ 4110 is relatively strong and the ratio is greater than 1.0, indicating a luminosity class of 0 (or brighter!). Note that this same effect is seen in the spectrum of two other carbon-rich PPNs, IRAS 22272 + 5435 and 05113 + 1347 (Hrivnak 1995).

We want to emphasize that the above high luminosity classes for these objects do not mean that they are intrinsically very luminous stars, which have high masses. Instead, they reflect the low surface gravity in these objects, which are low- or intermediate-mass stars with extended atmospheres and approximately a factor of 10 less luminous than supergiants of similar luminosity class.

It is interesting to note that the corresponding $T_{\text{eff}} = 5100$ K for 05341 + 0852 is significantly less than the value of 6500 K determined recently in an abundance study based on high-resolution spectra (Reddy et al. 1997). A similar discrepancy between the T_{eff} determined from low-resolution spectra and from abundance analyses using high-resolution spectra has also recently been noted for two other carbon-rich PPNs (Decin et al. 1998). These systematic differences suggest that the temperatures determined from an analysis of high-resolution spectra of IRAS Z02229 + 6208 and 07430 + 1115 will be higher than those based on the above spectral classifications. Such discrepancies may indicate that effective temperatures derived from solar abundance spectral standards may not be appropriate for these stars.

4.2. C_2 and C_3

The Swan bands of molecular C_2 at λ 4737 and λ 4715 are seen in the spectra of all three of these sources, as shown in Figure 6. They are strong in IRAS Z02229 + 6208 and 07430 + 1115 and weak in 05341 + 0852. The C_2 bands at λ 5165 and λ 5129 are very strong in Z02229 + 6208, strong in 07430 + 1115, and appear to be absent or very weak in 05341 + 0852, where we see instead the Mg b triplet. We also see the C_2 band head at λ 5635 in Z02229 + 6208. In our previous study of carbon-rich PPNs (Hrivnak 1995), we had found a general trend of stronger C_2 absorption bands with later spectral types; the results for these three additional sources conform to this trend.

The discovery of C_3 in PPNs came as a surprise (Hrivnak & Kwok 1991; Hrivnak 1995), although it had earlier been reported in the PPN AFGL 2688 (Egg Nebula; Crampton, Cowley, & Humphreys 1975). It is clearly seen in all three of these sources at λ 4051, λ 3992, λ 3916, and perhaps λ 3950

(see Fig. 7). The lines at λ 4051 and λ 3992 are strong in all three, as had been found in our previous study of carbon-rich PPNs. We now clearly identify the feature at λ 3916, which is seen in all three; in our previous study it was seen in AFGL 2688 and the early-G spectral type sources but not so clearly in the cooler ones. The C_3 feature at λ 3950 appears to be present in all three of these; a review of the spectra of the previously studied PPNs indicates that it may be present in some of these, but it is not seen as distinctly as in these three. The presence of C_3 in the optical spectra of stars continues to be rare, having been reported previously only for the late N-type carbon stars.

4.3. s -Process Elements

The s -process elements, formed from “slow” neutron capture, appear to be overabundant in these stars as compared with stars of solar composition. This is seen in the strengths of the Ba II lines at λ 4554 and λ 4934, Y II lines at λ 3983 and λ 4178, and Sr II at λ 4077. Since these are lines used in the luminosity classification, such an overabundance makes this classification less certain. This is a situation similar to what we found in our previous study of carbon-rich PPNs. A detailed abundance study is needed to quantify these results. Indeed, for 05341 + 0852, the high-resolution abundance study by Reddy et al. (1997) did find the s -process elements to be overabundant, $[s/\text{Fe}] \approx 2.2$. Similarly, for two other carbon-rich PPNs noted to appear to be overabundant in s -process elements (Hrivnak 1995), high-resolution abundance studies have supported this (Decin et al. 1998).

4.4. Miscellaneous Features

Additional strong lines are found in the spectra of these three PPNs, which we have not identified, but which seem useful to record. Features seen to be strong only in the three PPNs and not in the supergiant standards are found at λ 4021, λ 4971, λ 5293, and λ 5742. There are also some additional features seen to be strong in the three PPNs and also seen as strong in the two extremely luminous supergiants HD 4674 (G4 0-Ia) and ρ Cas (G2 0-Iae) but weak in less luminous supergiants (F5–K0 Ib). These are at the following wavelengths: λ 4110 (mentioned above), λ 4178 (mentioned above), λ 4352 (especially strong in 02229 + 6208), λ 4630, λ 4900, λ 4934 (which is strong, while λ 4938 is weak compared with the line in less luminous supergiants), λ 5382, and λ 5853. There is also a broad blend of several lines or what appears to be a band from λ 5473–5485 seen only in the PPNs.

5. SPECTRAL ENERGY DISTRIBUTIONS

Figure 2 shows the SEDs of IRAS Z02229 + 6208, 05341 + 0852, and 07430 + 1115. They all show “double-

perfect, provide us with clues to the conditions under which the 21 μm feature can form, which may aid us in the identification of the molecules involved.

The presence of molecular C_2 , C_3 , and CO all point to the fact that these are carbon-rich objects that have passed through the third dredge-up process. Their G and K spectral types and high luminosity class suggest that they are post-AGB objects evolving toward the PN stage. The SEDs of these objects show that the central stars of these objects were once embedded in the thick circumstellar dust envelopes of their AGB progenitors and are now just being seen again as the dust shell disperses. The emergence of PAH features and the unidentified 21 μm emission feature during this short transition phase suggests that complex carbon-based molecules can be synthesized in a low-density environment in timescales of several hundred years. This group of 12 carbon-rich post-AGB stars therefore makes

fascinating laboratories for the study of interstellar chemistry.

We thank T. Geballe for assisting in the UKIRT observations. The 1998 JCMT data were obtained as part of the JCMT service observing program. The assistance of T. Chester in reviewing the *IRAS* data on Z02229+6208 is much appreciated. B. E. Reddy assisted in the classification of the low-resolution spectra, and J. Ouyang assisted in the reduction of the SQUID data. We are grateful to the staff at UKIRT for the support of their service observing program; UKIRT is operated by the Royal Observatories on behalf of the UK Particle Physics and Astronomy Research Council. This research made use of the SIMBAD database, operated at CDS, Strasbourg, France. This work is supported in part by NSF (AST-9315107) and NASA/JOVE (NAG 8-232) grants to B. J. H. and an NSERC research grant to S. K.

REFERENCES

- Bakker, E. J., van Dishoeck, E. F., Waters, L. B. F. M., & Schoenmaker, T. 1997, *A&A*, 323, 469
- Bakker, E. J., Waters, L. B. F. M., Lamers, H. J. G. L. M., Trams, N. R., & Van der Wolf, F. L. A. 1996, *A&A*, 310, 893
- Burstein, D., & Heiles, C. 1982, *AJ*, 87, 1172
- Crampton, D., Cowley, A. P., & Humphreys, R. M. 1975, *ApJ*, 198, L135
- Decin, L., Van Winckel, H., Waelkens, C., & Bakker, E. J. 1998, *A&A*, 332, 928
- Elias, J. H., Frogel, J. A., Matthews, K., & Neugebauer, G. 1982, *AJ*, 87, 1029
- Geballe, T. R., & van der Veen, W. E. C. J. 1990, *A&A*, 235, L9
- Hrivnak, B. J. 1995, *ApJ*, 438, 341
- . 1997, in *IAU Symp. 180, Planetary Nebulae*, ed. H. J. Habing & H. Lamers (Dordrecht: Kluwer), 303
- Hrivnak, B. J., & Kwok, S. 1991, *ApJ*, 371, 363
- Hrivnak, B. J., Kwok, S., & Geballe, T. R. 1994, *ApJ*, 420, 783
- Hrivnak, B. J., Kwok, S., & Volk, K. 1989, *ApJ*, 346, 265
- Hrivnak, B. J., Volk, K., & Kwok, S. 1998, in *ISO's View of Stellar Evolution*, ed. L. B. F. M. Waters, C. Waelkens, & K. A. van der Hucht (Dordrecht: Kluwer), 477
- Jaschek, C., & Jaschek, M. 1987, *The Classification of Stars* (Cambridge: Cambridge Univ. Press)
- Justtanont, K., Barlow, M. J., Skinner, C. J., Roche, P. F., Aitken, D. K., & Smith, C. H. 1996, *A&A*, 309, 612
- Keenan, P. C., & McNeil, R. C. 1976, *An Atlas of Spectra of the Cooler Stars: Types G, K, M, S, and C* (Columbus: Ohio State Univ. Press)
- Kwok, S. 1993, *ARA&A*, 31, 63
- Kwok, S., Hrivnak, B. J., & Geballe, T. R. 1995, *ApJ*, 454, 394
- Kwok, S., Hrivnak, B. J., Zhang, C. Y., & Langill, P. L. 1996, *ApJ*, 472, 287
- Kwok, S., Volk, K., & Bidelman, W. 1997, *ApJS*, 112, 557
- Kwok, S., Volk, K., & Hrivnak, B. J. 1989, *ApJ*, 345, L51
- Landolt, A. U. 1983, *AJ*, 88, 439
- Lewis, B. M., Eder, J., & Terzian, Y. 1990, *ApJ*, 362, 634
- Manchado, A., Pottasch, S. E., Garcia-Lario, P., Esteban, C., & Mampaso, A. 1989, *A&A*, 214, 139
- Mosher, M., et al. 1992, *Explanatory Supplement to the IRAS Faint Source Survey, Version 2*, JPL D-10015 8/92 (Pasadena: JPL)
- Nickel, Th., & Klare, G. 1980, *A&AS*, 42, 251
- Nyman, L.-Å., et al. 1992, *A&AS*, 93, 121
- Omont, A., Loup, C., Forveille, T., te Lintel Hekkert, P., Habing, H., & Sivagnanam, P. 1993, *A&A*, 267, 515
- Reddy, B. E., & Parthasarathy, M. 1996, *A&A*, 112, 2053
- Reddy, B. E., Parthasarathy, M., Gonzalez, G., & Bakker, E. J. 1997, *A&A*, 328, 331
- te Lintel Hekkert, P., Caswell, J. L., Habing, H., Haynes, R. F., & Norris, R. P. 1991, *A&AS*, 90, 327
- Yamashita, Y., Nariai, K., & Norimoto, Y. 1978, *An Atlas of Representative Stellar Spectra* (New York: Halsted)